PHYSICAL REVIEW B VOLUME 15, NUMBER 12 15 JUNE 1977

Coupled-cluster expansion applied to the electron gas: Inclusion of ring and exchange effects*

David L. Freeman†
Department of Physics, The University of Utah, Salt Lake City, Utah 84112
(Received 7 January 1977)

The coupled-cluster expansion (or the Coester-Kümmel-Čižek method) is applied to the correlation problem in the uniform electron gas. Coupled nonlinear integral equations are developed for ring summations and the analytic structure of the expansion coefficients is examined. To facilitate the solution of the equations a technique is introduced to reduce the dimensionality of the problem. Numerical solution of the equations enable the evaluation of both ring and exchange effects. The direct random-phase-approximation (RPA) energy agrees with other work to the accuracy of the calculation. The screened exchange energy is evaluated for the first time and contributes about 30% of the RPA energy. The resulting correlation energy compares favorably with recent calculations using a dielectric formulation over the range of metallic electron densities.

I. INTRODUCTION

Owing to its similarity to metals with nearly spherical Fermi surfaces and to the growing importance of local density functionals, the electron gas is one of the most widely studied of many-body systems. Essential to an accurate description of the electron gas is the inclusion of correlation effects. An exact treatment of the correlation terms is only possible when the electron density is very high or very low. For the physically important region of intermediate densities correlation contributions are either approximated or obtained by interpolation between the high- and low-density limiting results.

Many-body perturbation theory[1] has been frequently employed to study correlation contributions to the properties of the electron gas. The classic calculation of the high-density correlation energy by Gell-Mann and Brueckner[2] used perturbative methods and there have been recent attempts to use diagrammatic formulations to extend the results to the region of metallic electron densities.[3-5] One of the advantages to the perturbative approach is that the expansion in principle will converge to the exact result if all terms are included. In addition Monkhorst and Oddershede[6] have recently demonstrated that perturbation theory can be applied to the correlation problem in real crystals. Unfortunately, any meaningful and convergent calculation using perturbation theory must include summations to infinite order in the electron-electron interaction. This renders it difficult to choose a physical basis from which to decide the appropriate terms to sum in the region of intermediate densities.

Some of the more successful investigations of correlation effects in the electron gas have used a dielectric formulation of the problem.[7-9] This approach has been very fruitful in describing the essential features of the system. One of the shortcomings of the dielectric method is that its connection with many-body perturbation theory is unclear. As a consequence the appropriate corrections to any given calculation are difficult to determine. In addition, as Singal and Das[10] have indicated, dielectric methods may be well suited for the electron gas but may not be useful for real crystals.

An expansion which can be expected to overcome the major deficiencies of both the dielectric method and perturbation theory is the coupled-cluster expansion, which has been alternatively called coupled-pair many-electron theory,[11-14] or the exp(S) method.[15-17] It is a rigorous expansion for the correlation correction, and the connection between the coupled-cluster method and the Goldstone expansion can be made clear. It is a useful expansion for real crystals, and it yields convergent, meaningful results in each order of truncation. One of the most appealing features of the method is that in its lowest orders (the T_2 approximation; see Sec. II B) ring diagrams are included simultaneously with particle-particle, hole-hole, and hole-particle ladder diagrams. These Goldstone diagrams have been speculated to have major importance for the electron gas. In spite of the power of the method there have only been a limited number of applications to electronic systems. The only application to the electron gas has been the work of Singal and Das[10] who included a class of diagrams which in atomic and molecular calculations has been called rearrangements.[18] Singal and Das obtained good agreement with the dielectric calculations for intermediate densities. For relatively high densities their results were less accurate apparently due to the neglect of ring diagrams.[19,20]

What follows is the first in a series of calculations on the correlation energy of the electron gas

using the coupled-cluster method. We begin by summing ring effects which are a necessary starting point for any calculation. Using the ring summations we evaluate both the random-phase-approximation (RPA) and screened exchange correlation energy. We also develop some of the analytic properties of the coefficients of the coupled-cluster expansion which will be essential for our subsequent work.

In Sec. II we develop the theory. The results are given in Sec. III and a discussion of the future direction of our work will be given in Sec. IV.

II. THEORY

In this section we present the theoretical details for applying the coupled-cluster expansion to the correlation problem in the electron gas. To introduce the necessary notation and to bring out some of the differences between the present formalism and perturbation theory, we begin by briefly describing the system.

A. Definition of the problem

We consider N electrons enclosed in a box of volume Ω. We shall study this system in the thermodynamic limit, i.e., where we allow both N and Ω to become infinite such that the density ρ defined by

$$\rho = N/\Omega \tag{1}$$

remains constant. To insure charge neutrality and to remove certain divergences that arise, we embed the system in a uniform background of positive charge of density ρ. As in other treatments of the electron gas it is convenient to write the Hamiltonian for this system as

$$H = H_0 + H' , \tag{2}$$

where

$$H_0 = -\frac{1}{2}\sum_i \nabla_i^2 \tag{3}$$

and

$$H' = \sum_{i<j}\sum_{\vec{k}\neq 0} \frac{4\pi}{\Omega k^2} e^{i\vec{k}\cdot(\vec{r}_i - \vec{r}_j)} . \tag{4}$$

Equation (4) is the Fourier expansion of the electron-electron interaction, and as is well known, the exclusion $\vec{k}\neq 0$ arises from divergences cancelling with contributions from the uniform background of positive charge. Unlike perturbation theory, in the treatment which follows it is unnecessary to rescale the Hamiltonian in terms of an expansion parameter depending on the density. As in many treatments it is convenient to describe a zeroth order approximation to the system in terms of the eigenfunctions of H_0. We write

$$H_0 = \sum_i h(\vec{r}_i) , \tag{5}$$

where

$$h(\vec{r}_i) = -\tfrac{1}{2}\nabla_i^2 . \tag{6}$$

The eigenfunctions of $h(\vec{r}_i)$ are given by

$$h(\vec{r}_i)\phi_{\vec{k}}^{\vec{k}}(\vec{r}_i) = \epsilon_{\vec{k}}^{\vec{k}}\phi_{\vec{k}}^{\vec{k}}(\vec{r}_i) , \tag{7}$$

where

$$\phi_{\vec{k}}^{\vec{k}}(\vec{r}_i) = [1/(\Omega)^{1/2}]\, e^{i\vec{k}\cdot\vec{r}_i} \tag{8}$$

and

$$\epsilon_{\vec{k}}^{\vec{k}} = \tfrac{1}{2}k^2 . \tag{9}$$

The ground-state eigenfunction of H_0, Φ_0, is a Slater determinant made by doubly occupying the $\frac{1}{2}N$ eigenfunctions of Eq. (7) which are lowest in energy. The highest-energy occupied state, called the Fermi level, has wave vector k_F. In terms of the electron density of the system, k_F is given by

$$k_F = (3\pi^2\rho)^{1/3} . \tag{10}$$

It is also convenient to define the classical electron radius for the system

$$r_s = (\tfrac{9}{4}\pi)^{1/3} k_F^{-1} . \tag{11}$$

We also define

$$E_0 = \langle \Phi_0 | H | \Phi_0 \rangle , \tag{12}$$

which is shown in a variety of text books[21] to be given by

$$E_0 = 2.20/r_s^2 - 0.916/r_s . \tag{13}$$

The energy in Eq. (13) is expressed in rydbergs per electron. In this paper we address the calculation of the correlation energy of the system ΔE which is defined by

$$\Delta E = E - E_0 , \tag{14}$$

where E is the exact ground-state energy of the system.

B. Coupled-cluster expansion

The theoretical method we use has been called alternatively, coupled-pair many-electron theory[11-14] or the exp(S) method.[15-17] The various developments of the method are equivalent. Because we wish to compare the calculations which follow with Goldstone diagrammatic perturbation theory,[1] we find it convenient to use the notation and development introduced by Čížek[11] for atomic and molecular problems and recently employed for the electron gas by Singal and Das.[10] The complete details concerning the diagrammatic

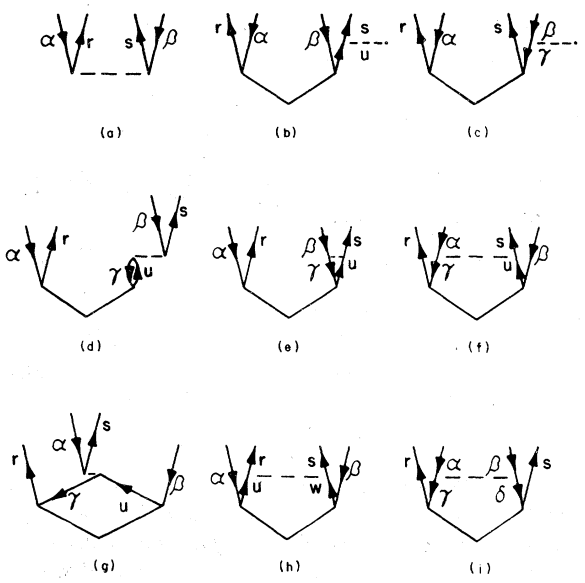

FIG. 1. Linear diagrams contributing in the T_2 approximation.

method can be found in Ref. 11. Here we sketch the necessary notational details.

The exact ground-state many-electron wave function, Ψ, for the electron gas satisfies the Schrödinger equation

$$H\Psi = E\Psi . \tag{15}$$

In the coupled-cluster method, we write

$$\Psi = e^{T}\Phi_0 , \tag{16}$$

where the operator T is given by

$$T = \sum_{j=1}^{N} T_j . \tag{17}$$

In Eq. (17) each T_j contribution is given by

$$T_j = \frac{1}{j!} \sum_{\substack{\alpha_1,\ldots,\alpha_j \\ r_1,\ldots,r_j}} t^{r_1,\ldots,r_j}_{\alpha_1,\ldots,\alpha_j} \prod_{i=1}^{j} C^{\dagger}_{r_i} C_{\alpha_i} , \tag{18}$$

where $C^{\dagger}_{r_i}, C_{\alpha_i}$ are, respectively, the creation operator for particle state r_i and the annihilation operator for hole state α_i and $t^{r_1,\ldots,r_j}_{\alpha_1,\ldots,\alpha_j}$ is an appropriate coefficient. In Eq. (18) and throughout this paper we have used the notation that Greek letters signify states occupied in Φ_0 and Latin letters signify virtual states. The coefficients in Eq. (18) are determined by a set of coupled equations. These equations are given diagrammatically in Ref. 11. To find the appropriate set of equations for our purposes it is useful to introduce an approximation to T. This approximation, used by Čížek[11,14] in atomic and molecular calculations, is given by

$$T \approx T_2 . \tag{19}$$

We shall call Eq. (19) the *T_2 approximation*. The diagrams corresponding to Eq. (19) are given in Figs. 1 and 2. They have been drawn in accordance with the rules given in Ref. 11 except that they are rotated by 90° to more easily see the connection with Goldstone theory.

Using the rules given in Ref. 11, and Eq. (7), the

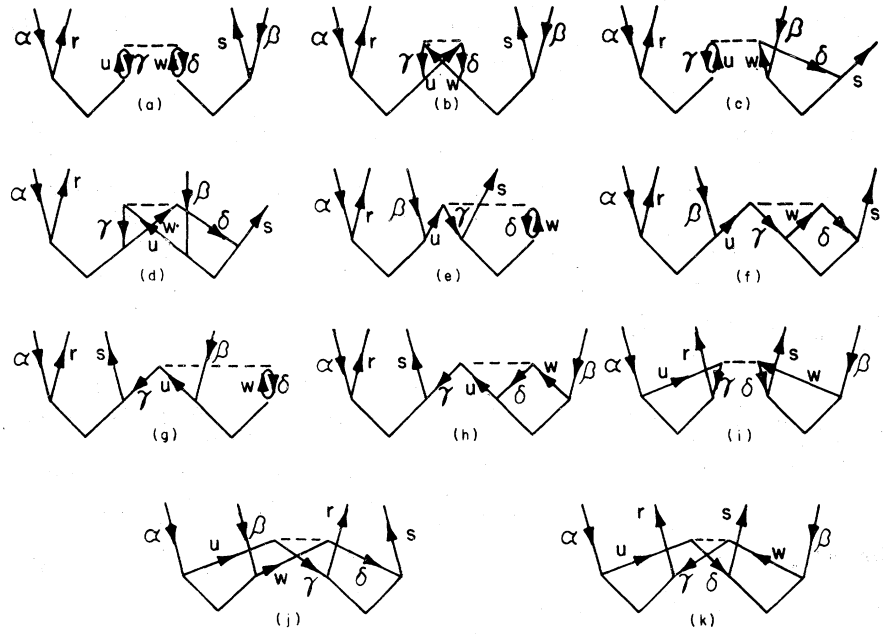

FIG. 2. Nonlinear diagrams contributing in the T_2 approximation.

T_2 equations are

$$t^{rs}_{\alpha\beta} = \frac{1}{\epsilon_\alpha+\epsilon_\beta-\epsilon_r-\epsilon_s}\Big(\langle rs|v|\alpha\beta\rangle + \sum_{\gamma u}(\langle\gamma s|v|\tilde{u}\beta\rangle t^{ru}_{\alpha\gamma} + \langle\gamma r|v|\tilde{u}\alpha\rangle t^{su}_{\beta\gamma} - \langle\gamma s|v|\alpha u\rangle t^{ru}_{\gamma\beta} - \langle\gamma r|v|\beta u\rangle t^{su}_{\gamma\alpha} - \langle\gamma s|v|u\alpha\rangle t^{ru}_{\gamma\beta} - \langle\gamma r|v|u\beta\rangle t^{su}_{\gamma\alpha}) + \sum_{uw}\langle rs|v|uw\rangle t^{uw}_{\alpha\beta} + \sum_{\gamma\delta}\langle\gamma\delta|v|\alpha\beta\rangle t^{rs}_{\gamma\delta} + \sum_{\gamma\delta uw}[\langle\gamma\delta|v|\tilde{uw}\rangle(t^{ru}_{\alpha\gamma}t^{sw}_{\beta\delta} + t^{su}_{\beta\gamma}t^{rw}_{\alpha\delta} - t^{ru}_{\alpha\gamma}t^{ws}_{\beta\delta} - t^{su}_{\beta\gamma}t^{wr}_{\alpha\delta} - t^{ru}_{\alpha\beta}t^{sw}_{\gamma\delta} - t^{su}_{\beta\alpha}t^{rw}_{\gamma\delta} - t^{rs}_{\alpha\gamma}t^{uw}_{\beta\delta} - t^{sr}_{\beta\gamma}t^{uw}_{\alpha\delta}) + \langle\gamma\delta|v|uw\rangle(t^{ur}_{\alpha\gamma}t^{sw}_{\delta\beta} + t^{uw}_{\alpha\beta}t^{rs}_{\gamma\delta}) + \langle\gamma\delta|v|wu\rangle t^{ur}_{\alpha\gamma}t^{sw}_{\delta\beta}]\Big). \tag{20}$$

In Eq. (20) the summations are taken over spin orbitals, v is the electron-electron interaction, and

$$\langle rs|v|\tilde{\alpha\beta}\rangle = \langle rs|v|\alpha\beta\rangle - \langle rs|v|\beta\alpha\rangle \tag{21}$$

is an antisymmetrized matrix element.

For the electron gas the matrix elements are labeled by their wave vector. We write

$$\langle\vec{k}_r\vec{k}_s|v|\vec{k}_\alpha\vec{k}_\beta\rangle = (4\pi/\Omega|\vec{k}_r-\vec{k}_\alpha|^2)\delta_{\vec{k}_r-\vec{k}_\alpha,\vec{k}_\beta-\vec{k}_s} = (4\pi/\Omega q^2)\delta_{\vec{k}_r-\vec{k}_\alpha,\vec{k}_\beta-\vec{k}_s}, \tag{22}$$

where $\vec{q}$, given by

$$\vec{q} = \vec{k}_r - \vec{k}_\alpha, \tag{23}$$

is the momentum transferred by the Coulomb interaction.

Equation (20) gives the appropriate expansion coefficients for the many-electron wave function through Eq. (16). The correlation energy is obtained by evaluating the diagrams given in Fig. 3. The direct diagram [Fig. 3(a)] gives

$$\Delta E_{\rm dir} = \sum_{rs\alpha\beta}\langle rs|v|\alpha\beta\rangle t^{rs}_{\alpha\beta} \tag{24}$$

and the exchange diagram [Fig. 3(b)] contributes

$$\Delta E_{\rm ex} = -\sum_{rs\alpha\beta}\langle rs|v|\beta\alpha\rangle t^{rs}_{\alpha\beta}. \tag{25}$$

As in Eq. (20) the summations are taken over spin orbitals.

As was indicated in Ref. 11 it is possible to sum a class of Goldstone diagrams by solving the equations resulting from evaluating particular diagrams from Figs. 1 and 2. For example, if we include diagrams (a)– (d) from Fig. 1 and (a) from Fig. 2, we will have an equation which is equivalent to summing all the Goldstone ring diagrams. This can be proved by choosing the appropriate terms from Eq. (20) and iterating the equation for $t^{rs}_{\alpha\beta}$. As is well known, inclusion of the ring diagrams is essential to remove the divergences in the order by order Goldstone expansion.[21] We now examine the ring equations in some detail.

C. Ring equations

By virtue of Eq. (22) the t coefficients for the electron gas will depend only on two wave vectors and the momentum transferred. We let

$$t_q(\vec{k}_i,\vec{k}_j) = t^{\vec{k}_i+\vec{q},\vec{k}_j-\vec{q}}_{\vec{k}_i,\vec{k}_j}, \tag{26}$$

so that

$$T_2 = \sum_{\vec{k}_i,\vec{k}_j,\vec{q}} t_q(\vec{k}_i,\vec{k}_j)C^\dagger_{\vec{k}_i+\vec{q}}C^\dagger_{\vec{k}_j-\vec{q}}C_{\vec{k}_j}C_{\vec{k}_i}. \tag{27}$$

If we write the solution to the equations for the ring diagrams as $t^R_q(\vec{k}_i,\vec{k}_j)$, by choosing the appropriate terms from Eq. (20) we obtain

$$t^R_q(\vec{k}_i,\vec{k}_j) = \frac{4\pi}{D_q(\vec{k}_i,\vec{k}_j)\Omega q^2}\Big(1 + \sum_{\vec{k},\sigma}[t^R_q(\vec{k}_i,\vec{k}) + t^R_q(\vec{k}_j,\vec{k})]\,\theta(\vec{k})[1-\theta(\vec{k}+\vec{q})] + \frac{1}{2}\sum_{\vec{k},\sigma}\sum_{\vec{k}',\sigma}[t^R_q(\vec{k}_i,\vec{k})t^R_q(\vec{k}_j,\vec{k}') + t^R_q(\vec{k}_i,\vec{k}')t^R_q(\vec{k}_j,\vec{k})]\,\theta(\vec{k})\theta(\vec{k}')[1-\theta(\vec{k}+\vec{q})][1-\theta(\vec{k}'+q)]\Big), \tag{28}$$

where $D_q(\vec{k}_i,\vec{k}_j)$ is the energy denominator given by

$$D_q(\vec{k}_i,\vec{k}_j) = -[q^2 + \vec{q}\cdot(\vec{k}_i+\vec{k}_j)], \tag{29}$$

$\theta(\vec{k})$ is a Pauli exclusion factor given by

$$\theta(\vec{k}) = \begin{cases} 0, & |\vec{k}| > k_F, \\ 1, & |\vec{k}| < k_F, \end{cases} \tag{30}$$

and the σ denotes the spin quantum numbers.

In the thermodynamic limit we may replace the summations in Eq. (28) by integrations using the relation

$$\sum_{\vec{k}} \to \frac{\Omega}{(2\pi)^3}\int d^3k . \tag{31}$$

If we also perform the integration in units of k_F, and define

$$\eta(\vec{k}) = \begin{cases} 1, & |\vec{k}|<1 , \\ 0, & |\vec{k}|>1 , \end{cases} \tag{32}$$

we obtain

$$t_q^R(\vec{k}_i,\vec{k}_j) = \frac{4}{3\pi k_F q^2 D_q(\vec{k}_i,\vec{k}_j)}\Big(1+6\pi^2\int\frac{d^3k}{(2\pi)^3}[t_q^R(\vec{k}_i,\vec{k})+t_q^R(\vec{k}_j,\vec{k})]\eta(\vec{k})[1-\eta(\vec{k}+\vec{q})]$$
$$+18\pi^4\int\frac{d^3k}{(2\pi)^3}\int\frac{d^3k'}{(2\pi)^3}[t_q^R(\vec{k}_i,\vec{k})t_q^R(\vec{k}_j,\vec{k}')+t_q^R(\vec{k}_i,\vec{k}')t_q^R(\vec{k}_j,\vec{k})]\eta(\vec{k})\eta(\vec{k}')$$
$$\times[1-\eta(\vec{k}+\vec{q})][1-\eta(\vec{k}'+\vec{q})]\Big) \tag{33}$$

In Eq. (33) we have performed the necessary summations over spin. We note that Eq. (33) makes manifest the well-known result that ring diagrams do not couple different components of the momentum transferred. We can solve Eq. (33) for each value of q separately.

For our future discussions it is useful to note that Eq. (33) contains both linear and nonlinear parts. The linear part can be solved separately using the equation

$$t_q^{FR}(\vec{k}_i,\vec{k}_j) = \frac{4}{3\pi k_F q^2 D_q(\vec{k}_i,\vec{k}_j)}\Big(1+6\pi^2\int\frac{d^3k}{(2\pi)^3}[t_q^{FR}(\vec{k}_i,\vec{k})+t_q^{FR}(\vec{k}_j,\vec{k})]\eta(\vec{k})[1-\eta(\vec{k}+\vec{q})]\Big) . \tag{34}$$

The difference between $t_q^R(\vec{k}_i,\vec{k}_j)$ and $t_q^{FR}(\vec{k}_i,\vec{k}_j)$ is clearly the nonlinear contributions. The effect of the nonlinear terms can be seen in Fig. 4. The linear part contains the forward time ordered Goldstone ring diagrams like those shown in Figs. 4(a) and 4(b), whereas the nonlinear terms introduce the other time orderings like that shown in Fig. 4(c).

The regions of integration in Eqs. (33) and (34) are depicted in Fig. 5 as the region outside sphere A and inside sphere B. The centers of spheres A and B are separated by q. There are four cases for the limits on the $\vec{k}$ integration; one for $q<1$, the next for $1<q<\sqrt{2}$, the next for $\sqrt{2}<q<2$ and the last for $q<2$. The first three cases are shown in Fig. 5. The appropriate limits on the $\vec{k}$ integration for the case depicted in Fig. 5(a) are

θ: $[0, \pi-\tan^{-1}\{2(1-\frac{1}{4}q^2)^{1/2}/q\}]$,

k: $[-q\cos\theta+(1-q^2\sin^2\theta)^{1/2}, 1]$.

For the case depicted in Fig. 5(b) there are three regions of integration, labeled in the figure as I, II, and III. The limits of integration are

k: $[0,1]$,

θ: $[0, \frac{1}{2}\pi+\tan^{-1}\{(q^2-1)^{1/2}\}]$

for region I;

θ: $[\frac{1}{2}\pi+\tan^{-1}\{(q^2-1)^{1/2}\}, \ \pi-\tan^{-1}\{2(1-\frac{1}{4}q^2)^{1/2}/q\}]$,

k: $[-q\cos\theta-\cos\theta\{q^2-\sec^2\theta(q^2-1)\}^{1/2}, 1]$

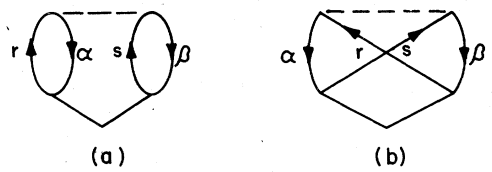

FIG. 3. (a) Direct energy diagram; (b) the exchange energy diagram.

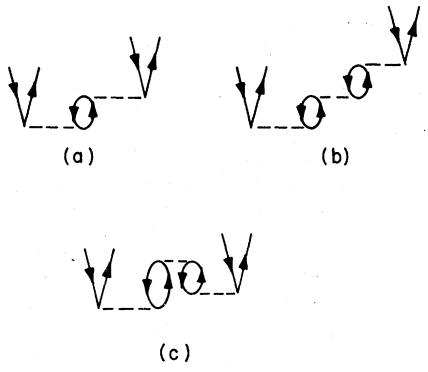

FIG. 4. (a) and (b) examples of forward time-ordered Goldstone ring diagrams included in the linear part of Eq. (33); (c) an example of the other time orderings arising from the nonlinear part of Eq. (33).

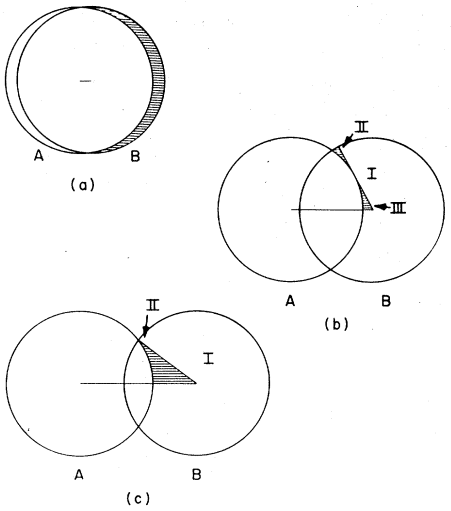

FIG. 5. Regions of $\vec{k}$ integration are shown as the region outside sphere A and inside sphere B for (a) $q<1$, (b) $1<q<\sqrt{2}$, and (c) $\sqrt{2}<q<2$ for q measured in units of k_F.

for region II; and

$$\theta\colon\ [\tfrac{1}{2}\pi+\tan^{-1}\{(q^2-1)^{1/2}\},\pi],$$

$$k\colon\ [0,-q\cos\theta+\cos\theta\{q^2-\sec^2\theta(q^2-1)\}^{1/2}]$$

for region III.

For the case shown in Fig. 5(c) there are two regions labeled I and II. For region I the limits are

$$k\colon\ [0,1],$$

$$\theta\colon\ [0,\pi-\tan^{-1}\{2(1-\tfrac{1}{4}q^2)^{1/2}/q\}],$$

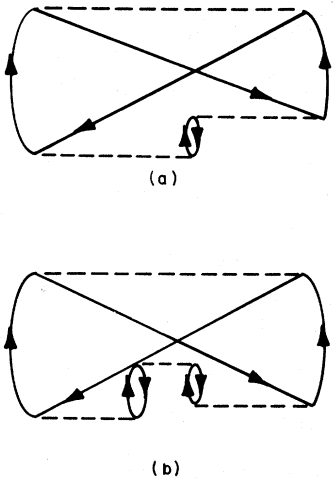

FIG. 6. Screened exchange diagrams included in Eq. (36).

and the limits for region II are

$$\theta\colon\ [\pi-\tan^{-1}\{2(1-\tfrac{1}{4}q^2)^{1/2}/q\},\pi],$$

$$k\colon\ [0,-q\cos\theta+\cos\theta\{q^2-\sec^2\theta(q^2-1)\}^{1/2}].$$

When $q>2$ the integration on $\vec{k}$ is over a sphere of radius 1.

For the ring summation the electron gas has azimuthal symmetry and the integration over the ϕ coordinate will give a factor of 2π. As we shall see in subsequent work this symmetry property is not present for correlation calculations that go beyond the rings and limits on the ϕ integrations will be needed.

Using Eqs. (22), (24)–(26), (31), and (32) we obtain energy expressions

$$\Delta E^R_{\rm dir}=144\pi^5 k_F\int\frac{d^3q}{(2\pi)^3}\int\frac{d^3k_i}{(2\pi)^3}\int\frac{d^3k_j}{(2\pi)^3}\frac{1}{q^2}\,t^R_q(\vec{k}_i,\vec{k}_j)\eta(\vec{k}_i)\eta(\vec{k}_j)[1-\eta(\vec{k}_i+\vec{q})][1-\eta(\vec{k}_j+\vec{q})] \tag{35}$$

and

$$\Delta E^R_{\rm ex}=-72\pi^5 k_F\int\frac{d^3k_i}{(2\pi)^3}\int\frac{d^3k_j}{(2\pi)^3}\int\frac{d^3q}{(2\pi)^3}\,t^R_q(\vec{k}_i,\vec{k}_j)\frac{1}{(\vec{k}_i+\vec{k}_j+\vec{q})^2}\,\eta(\vec{k}_i)\eta(\vec{k}_j)[1-\eta(\vec{k}_i+\vec{q})][1-\eta(\vec{k}_j+\vec{q})], \tag{36}$$

where the units in Eqs. (35) and (36) are in rydbergs per electron. There are expressions analogous to Eqs. (35) and (36) for the energy including only forward time ordered ring contributions. They are obtained from Eqs. (35) and (36) by replacing $t^R_q(\vec{k}_i,\vec{k}_j)$ by $t^{FR}_q(\vec{k}_i,\vec{k}_j)$. For our future discussions we shall denote the forward time-ordered direct and exchange correlation energy, respectively, as $\Delta E^{FR}_{\rm dir}$ and $\Delta E^{FR}_{\rm ex}$.

The direct contribution to the correlation energy [Eq. (35)] is often called the random-phase approximation (RPA).[21] The exchange energy [Eq. (36)] includes screened exchange effects as well as the second-order Goldstone exchange contribution. In Fig. 6 we give examples of screened exchange Goldstone diagrams included in Eq. (36).

In the form of Eq. (33) the ring equations are difficult to solve because $t^R_q(\vec{k}_i,\vec{k}_j)$ defines a five-dimensional matrix. To reduce the dimensionality of the equations it is convenient to define

$$T_q(\vec{k}_i)=\int\frac{d^3k}{(2\pi)^3}\,t^R_q(\vec{k}_i,\vec{k})\eta(\vec{k})[1-\eta(\vec{k}+\vec{q})]. \tag{37}$$

Then Eq. (33) becomes

$$t_q^R(\vec{k}_i,\vec{k}_j)=[4/3\pi k_F q^2 D_q(\vec{k}_i,\vec{k}_j)] \times\{1+6\pi^2[T_q(\vec{k}_i)+T_q(\vec{k}_j)]+36\pi^4 T_q(\vec{k}_i)T_q(\vec{k}_j)\}. \tag{38}$$

We shall now use Eq. (38) to find an integral equation for $T_q(\vec{k}_i)$. This equation, when solved, directly yields $t_q^R(\vec{k}_i,\vec{k}_j)$ by substitution into Eq. (38). We integrate both sides of Eq. (38) over $\vec{k}_j$ and obtain

$$T_q(\vec{k}_i)=\int \frac{d^3k_j}{(2\pi)^3}\eta(\vec{k}_j)[1-\eta(\vec{k}_j+\vec{q})]\frac{4}{3\pi k_F q^2 D_q(\vec{k}_i,\vec{k}_j)}\{1+6\pi^2[T_q(\vec{k}_i)+T_q(\vec{k}_j)]+36\pi^4 T_q(\vec{k}_i)T_q(\vec{k}_j)\}. \tag{39}$$

Analogous expressions can be derived for the linear equations by using Eq. (34). We obtain

$$T_q^{FR}(\vec{k}_i)=\int \frac{d^3k}{(2\pi)^3}\eta(\vec{k})[1-\eta(\vec{k}+\vec{q})]\frac{4}{3\pi k_F q^2 D_q(\vec{k}_i,\vec{k})}\{1+6\pi^2[T_q^{FR}(\vec{k}_i)+T_q^{FR}(\vec{k})]\} \tag{40}$$

and

$$t_q^{FR}(\vec{k}_i,\vec{k}_j)=[4/3\pi k_F q^2 D_q(\vec{k}_i,\vec{k}_j)]\{1+6\pi^2[T_q^{FR}(\vec{k}_i)+T_q^{FR}(\vec{k}_j)]\}. \tag{41}$$

To find a numerical solution to Eq. (39) [or in a similar manner to Eq. (40)] we introduce a quadrature formula to perform the integrations. If we write

$$\int \frac{d^3k}{(2\pi)^3}\eta(\vec{k})[1-\eta(k+\vec{q})]\to\sum_{\vec{k}} W_{\vec{k}}, \tag{42}$$

where $W_{\vec{k}}$ are quadrature weights, we obtain

$$T_q(\vec{k}_i)\left(1-\frac{8\pi}{k_F q^2}\sum_{\vec{k}} W_{\vec{k}}\frac{1}{D_q(\vec{k}_i,\vec{k})}\right)-\frac{8\pi}{k_F q^2}\sum_{\vec{k}} W_{\vec{k}}\frac{1}{D_q(\vec{k}_i,\vec{k})}T_q(\vec{k}) =\frac{4}{3\pi q^2 k_F}\sum_{\vec{k}}\frac{W_{\vec{k}}}{D_q(\vec{k}_i,\vec{k})}+\frac{48\pi^3}{k_F q^2}T_q(\vec{k}_i)\sum_{\vec{k}} W_{\vec{k}}\frac{T_q(\vec{k})}{D_q(\vec{k}_i,\vec{k})}. \tag{43}$$

It is convenient to introduce the notation

$$T_i=T_q(\vec{k}_i) \tag{44}$$

and

$$D_{ik}=\frac{4\pi}{q^2 D_q(\vec{k}_i,\vec{k})}. \tag{45}$$

Then Eq. (43) becomes

$$T_i\left(1-\frac{2}{k_F}\sum_m W_m D_{im}\right)-\frac{2}{k_F}\sum_k W_k D_{ik}T_k =\sum_m W_m\frac{D_{im}}{3\pi^2 k_F}+\frac{12\pi^2}{k_F}T_i\sum_m W_m T_m D_{im} \tag{46}$$

or

$$\sum_k\left[\delta_{ik}\left(1-\frac{2}{k_F}\sum_m W_m D_{im}\right)-\frac{2}{k_F}W_k D_{ik}\right]T_k =\sum_m W_m\left(\frac{D_{im}}{3\pi^2 k_F}+\frac{12\pi^2}{k_F}T_i T_m D_{im}\right). \tag{47}$$

If we write

$$A_{ik}=\delta_{ik}\left(1-\frac{2}{k_F}\sum_m W_m D_{im}\right)-\frac{2}{k_F}W_k D_{ik} \tag{48}$$

and

$$B_i=\sum_m W_m\left(\frac{D_{im}}{3\pi^2 k_F}+\frac{12\pi^2}{k_F}T_i T_m D_{im}\right), \tag{49}$$

then Eq. (47) becomes

$$\sum_k A_{ik}T_k=B_i. \tag{50}$$

We write this matrix equation as

$$\underline{A}\cdot\vec{T}=\vec{B}(\vec{T}). \tag{51}$$

The matrix equation can be solved by standard techniques. We note that the right-hand side of Eq. (51) depends on the solution vector $\vec{T}$ and that an iterative solution to Eq. (51) is required. An analogous set of equations can be found by introducing a quadrature formula into Eq. (40). The resulting equations are linear and no iterations are needed.

We shall discuss the numerical solution to the ring equations in Sec. III. We complete this section by examining the analytic structure of the coefficients of the expansion in the ring approximation.

D. Behavior of the coefficients

The following properties of the coefficients discussed in Sec. II C are important both for the numerical solution to the ring equations and for future applications of the formalism:

$$\lim_{q\to 0} T_q(\vec{k}_i) = -\frac{1}{6\pi^2}, \tag{52}$$

$$\lim_{q\to 0} T_q^{FR}(\vec{k}_i) = -\frac{1}{12\pi^2}, \tag{53}$$

$$\lim_{q\to 0} t_q^R(\vec{k}_i, \vec{k}_j) = f(\vec{k}_i, \vec{k}_j) q^{-1}, \tag{54}$$

where $f(\vec{k}_i, \vec{k}_j)$ is some function of $\vec{k}_i$ and $\vec{k}_j$;

$$\lim_{q\to\infty} t_q^R(\vec{k}_i, \vec{k}_j) = -\frac{4}{3\pi k_F q^4} \tag{55}$$

and

$$\lim_{q\to 2} \frac{\partial}{\partial q} \int d^3k_j \int d^3k_j\, t_q^R(\vec{k}_i, \vec{k}_j)\eta(\vec{k}_i) \times \eta(\vec{k}_j)[1-\eta(\vec{k}_i+q)][1-\eta(\vec{k}_j+q)] = \infty, \tag{56}$$

where q is expressed in units of k_F.

We can prove Eq. (52) if we rewrite Eq. (39) as

$$T_q(\vec{k}_i) = \left(\frac{4}{3\pi k_F q^2}\int \frac{d^3k}{(2\pi)^3}\frac{\eta(\vec{k})[1-\eta(\vec{k}+\vec{q})]}{D_q(\vec{k}_i,\vec{k})}\right)\Big/\left[1-\frac{8\pi}{q^2k_F}\int\frac{d^3k}{(2\pi)^3}\frac{\eta(\vec{k})[1-\eta(\vec{k}+\vec{q})]}{D_q(\vec{k}_i,\vec{k})}\left(1+\frac{T_q(\vec{k})}{T_q(\vec{k}_i)}\right) - \frac{48\pi^3}{k_F q^2}\int\frac{d^3k}{(2\pi)^3}\frac{\eta(\vec{k})[1-\eta(\vec{k}+\vec{q})]T_q(\vec{k})}{D_q(\vec{k}_i,\vec{k})}\right]. \tag{57}$$

We define

$$\alpha(q,\vec{k}_i) = \frac{4}{3\pi k_F q^2}\int\frac{d^3k}{(2\pi)^3}\frac{\eta(\vec{k})[1-\eta(\vec{k}+\vec{q})]}{D_q(\vec{k}_i,\vec{k})}. \tag{58}$$

As q approaches zero Eq. (57) becomes

$$\lim_{q\to 0} T_q(\vec{k}_i) = [\alpha^{-1}(q,\vec{k}_i) - 12\pi^2 - 36\pi^4 T_q(\vec{k}_i)]^{-1}, \tag{59}$$

where we have used the fact that $T_q(\vec{k}_i)$ is independent of $\vec{k}_i$ for small q. As q approaches zero $\alpha(q,\vec{k}_i)$ becomes infinite so that Eq. (59) becomes

$$\lim_{q\to 0} T_q(\vec{k}_i) = [-12\pi^2 - 36\pi^4 T_q(k_i)]^{-1}. \tag{60}$$

Solving Eq. (60) for $T_q(\vec{k}_i)$ we obtain Eq. (52). We can prove Eq. (53) in a similar manner.

We can use Eq. (52) to prove Eq. (54). From Eq. (37)

$$\lim_{q\to 0} T_q(\vec{k}_i) = \lim_{q\to 0}\int\frac{d^3k_j}{(2\pi)^3} t_q^R(\vec{k}_i,\vec{k}_j)\eta(\vec{k}_j)[1-\eta(\vec{k}_j+\vec{q})]. \tag{61}$$

Because $t_q(\vec{k}_i,\vec{k}_j)$ is a weak function of $\vec{k}_i$, and $\vec{k}_j$ for small q, we can approximate

$$\lim_{q\to 0} T_q(\vec{k}_i) \cong \lim_{q\to 0} t_q^R(k_i,k_j) \times\int\frac{d^3k_j}{(2\pi)^3}\eta(\vec{k}_j)[1-\eta(\vec{k}_j+\vec{q})]. \tag{62}$$

The volume of the integrated region is given by

$$V(q) = \int d^3k\,\eta(\vec{k})[1-\eta(\vec{k}+\vec{q})] = \pi(q-\tfrac{1}{12}q^3), \tag{63}$$

so that Eq. (62) becomes

$$\lim_{q\to 0} T_q(k_i) \cong \lim_{q\to 0} t_q^R(k_i,k_j)\frac{V(q)}{(2\pi)^3}, \tag{64}$$

or using Eqs. (52) and (63) we obtain

$$\lim_{q\to 0} t_q^R(\vec{k}_i,\vec{k}_j) \cong -\frac{4}{3q}. \tag{65}$$

The assumption that $t_q(\vec{k}_i,\vec{k}_j)$ is independent of $\vec{k}_i$ and $\vec{k}_j$ for small q is only approximately correct, so that Eq. (65) rigorously gives the correct q dependence of $t_q(\vec{k}_i,\vec{k}_j)$ and proves Eq. (54).

We can prove Eq. (55) by noting that the first term on the right-hand side of Eq. (33) is dominant as $q\to\infty$ and

$$\lim_{q\to\infty} D_q(\vec{k}_i,\vec{k}_j) = -q^2. \tag{66}$$

The slope discontinuity at $q=2$ [Eq. (56)] is similar to the slope discontinuity in the electron gas dielectric function. It occurs because the nature of the Pauli exclusion factors changes at $q=2$ and a discussion of the mathematical details can be found elsewhere.[22]

III. RESULTS

Gauss-Legendre quadrature was introduced into Eq. (39) to obtain Eq. (51). The values of q used in Eq. (51) were chosen to be the Gauss-Legendre grid required to accurately evaluate Eqs. (35) and (36). Because of the slope discontinuity [Eq. (56)] it was necessary to divide the region of the q integration into three sections. It was found that dividing the regions into [0, 1.95], [1.95, 2.05], and [2.05, ∞] was sufficiently accurate to evaluate the correlation energy to four significant figures. Twelve Gauss-Legendre points were used in the first region, two in the second, and 26 in the third.

The size of the mesh of points used for the k integrations [Eq. (39)] depended on the value of q. For the case that $q<1$, regions I and III for the case shown in Fig. 5(b), for regions I and II for the case shown in Fig. 5(c) and for $q>2$, four quad-

rature points were used for the k integration and four quadrature points were used in the θ integration. For region II in the case shown in Fig. 5(b) two quadrature points were used in the k integration and two quadrature points were used in the θ integration.

We first solved the linear part of the ring equations [Eq. (40)]. The linear equations were solved by standard techniques and the results are given in Table I. In Table I we have put

$$\Delta E^{FR} = \Delta E^{FR}_{\rm dir} + \Delta E^{FR}_{\rm ex} . \tag{67}$$

The significance of these results will be more transparent when we compare them with the full ring summation. It is useful to compare the exchange energy $\Delta E^{FR}_{\rm ex}$ with the second-order exchange Goldstone diagram which contributes 0.046 Ry and is r_s independent.[2] From Table I it is clear that the unscreened second-order exchange energy becomes unphysically large for large r_s. In contrast $\Delta E^{FR}_{\rm ex}$ contributes somewhat less than 50% of $\Delta E^{FR}_{\rm dir}$ for all r_s. This confirms the well-known fact that the unscreened second-order exchange energy overestimates the effect of exchange to the total correlation energy for low and intermediate electron densities. As r_s becomes small $\Delta E^{FR}_{\rm ex}$ approaches the bare second-order exchange result.

To solve the full ring equations [Eq. (39)] an iterative solution was required. Preliminary attempts to use $T^{FR}_q(\vec{k}_i)$ as the first guess resulted in poor convergence of the iterative equations. The convergence difficulties were particularly severe for small q where the solutions differ by a factor of 2 [see Eqs. (52) and (53)]. For large q, $T^{FR}_q(\vec{k}_i)$ and $T_q(\vec{k}_i)$ are identical. Numerical experience taught us that choosing

TABLE I. Forward time-ordered ring contribution to the correlation energy.[a]

r_s	$\Delta E^{FR}_{\rm dir}$[b]	$\Delta E^{FR}_{\rm ex}$[c]	ΔE^{FR}
1	−0.1462	0.03886	−0.1073
2	−0.1128	0.03432	−0.07848
3	−0.09512	0.03116	−0.06396
4	−0.08358	0.02876	−0.05482
5	−0.07522	0.02682	−0.04840
6	−0.06882	0.02520	−0.04362
7	−0.06368	0.02384	−0.03984
8	−0.05946	0.02266	−0.03680
9	−0.05590	0.02162	−0.03428
10	−0.05284	0.02070	−0.03214

[a] Rydberg units.
[b] Obtained from Eq. (35) by substituting $t^{FR}_q(\vec{k}_i,\vec{k}_j)$ for $t^R_q(\vec{k}_i,\vec{k}_j)$.
[c] Obtained from Eq. (36) by substituting $t^{FR}_q(\vec{k}_i,\vec{k}_j)$ for $t^R_q(\vec{k}_i,\vec{k}_j)$.

TABLE II. The correlation contribution from Eq. (51) as a function of the number of iterations for $r_s = 1$.[a]

No. of iterations	$\Delta E^R_{\rm dir}$	$\Delta E^R_{\rm ex}$	ΔE^R
1	−0.13730	0.03896	−0.09834
2	−0.14668	0.03922	−0.1075
3	−0.16084	0.03938	−0.1215
4	−0.15990	0.03936	−0.1205
5	−0.15932	0.03936	−0.1200
6	−0.15770	0.03936	−0.1183
7	−0.15768	0.03936	−0.1183
8	−0.15768	0.03936	−0.1183

[a] Rydberg units.

$$T_q(\vec{k}_i) = -(1-q)/6\pi^2 \tag{68}$$

for $q < 1$ and

$$T_q(\vec{k}_i) = 0 \tag{69}$$

for $q > 1$, as the first iterate provided satisfactory convergence. Additional improvement of the convergence properties was obtained by using a Shanks Transformation[23] on $\vec{B}(\vec{T})$.

The convergence properties of the equations can be seen in Table II. In Table II we have defined

$$\Delta E^R = \Delta E^R_{\rm dir} + \Delta E^R_{\rm ex} . \tag{70}$$

Convergence to four significant figures is attained in six iterations.

In Table III the correlation energy is given for r_s equal to 1–10. The results were computed with six iterations of Eq. (51). For comparison in the last column of Table III we give the calculations of Vashishta and Singwi[8] who used a dielectric formulation. Unlike the calculation of Gell-Mann and Brueckner[2] which gives the RPA energy as an expansion in r_s and is only valid in the high-density

TABLE III. Correlation energy of the electron gas as a function of r_s.[a]

r_s	$\Delta E^R_{\rm dir}$	$\Delta E^R_{\rm ex}$	ΔE^R	ΔE[b]
1	−0.1577	0.03936	−0.1183	−0.112
2	−0.1235	0.03512	−0.08838	−0.089
3	−0.1055	0.03218	−0.07332	−0.075
4	−0.09354	0.02994	−0.06360	−0.065
5	−0.08486	0.02814	−0.05672	−0.058
6	−0.07816	0.02664	−0.05152	−0.052
7	−0.07278	0.02534	−0.04744	
8	−0.06830	0.02424	−0.04406	
9	−0.06452	0.02324	−0.04128	
10	−0.06126	0.02238	−0.03888	

[a] Rydberg units.
[b] Reference 8.

limit, the direct energy given here is the exact RPA energy and agrees with the results of Hedin[24] to the accuracy of his calculation. As in the linear case the exchange energy is well behaved for large r_s in contrast to the unscreened second-order exchange energy. To our knowledge this is the first such calculation of this screened contribution to the exchange energy for the electron gas, and we find that it contributes about 30% of the RPA energy for all computed values of r_s. The agreement between ΔE^R and the results of Vashishta and Singwi[8] is excellent for all computed electron densities. By comparing Table III with Table I it is clear that the nonlinear terms are important and contribute between 10 and 20% of the total correlation energy.

IV. DISCUSSION

We have used the coupled-cluster expansion to sum ring effects in the electron gas. Using the ring summations we have evaluated both direct and exchange contributions to the correlation energy. The agreement between the calculated correlation correction and the results of recent self consistent dielectric function calculations was excellent.

This agreement does not imply that all important correlation effects have been included. We have neglected particle-particle ladder [Fig. 1(h)], hole-hole ladder [Fig. 1(i)], hole-particle ladder [Figs. 1(e)–1(g)], and nonlinear diagrams other than Fig 2(a), in addition to terms beyond the T_2 approximation. Recent calculations have emphasized the importance of some of the terms in the T_2 approximation that we have ignored,[5,10] and we intend to investigate them systematically. Of particular interest is a study of the effect of simultaneously summing particle-particle ladder and ring diagrams. Such a calculation is presently in progress, and will include both short and long-range correlations as well as allow comparison with the recent work of Lowy and Brown.[5] Future work will also study the contribution of rearrangement effects and particle-hole ladder diagrams.

It is important to note that nonlinear equations of the type we have investigated will have multiple solutions. The solution we found to Eq. (33) is not unique. Recent studies by Zivkovic and Monkhorst[25] have suggested that the other solutions may provide useful approximations for some of the excited states of the system. Since the excitation spectrum is of great interest, methods for finding the multiple solutions are in progress. Additional work on other properties of the electron gas is also anticipated.

ACKNOWLEDGMENTS

Many thanks go to Professor F. E. Harris and Professor H. J. Monkhorst for invaluable and stimulating discussions and continuing encouragement throughout the course of this work. Useful discussions with Dr. R. Ault, Dr. L. Kumar, and J. Pack on the numerical aspects of this work are also gratefully acknowledged.

---

*Supported in part by the U.S. NSF Grant No. CHE-7501284.

†Present address: Department of Chemistry, The University of Rhode Island, Kingston, Rhode Island 02881.

[1]J. Goldstone, Proc. R. Soc. A 239, 267 (1957).
[2]M. Gell-Mann and K. A. Brueckner, Phys. Rev. 106, 364 (1957).
[3]H. Yasuhara, Solid State Commun. 11, 1481 (1972).
[4]B. B. J. Hede and J. P. Carbotte, Can. J. Phys. 50, 1756 (1972).
[5]D. N. Lowy and G. E. Brown, Phys. Rev. B 12, 2138 (1975).
[6]H. J. Monkhorst and J. Oddershede, Phys. Rev. Lett. 30, 797 (1973).
[7]K. S. Singwi, A. Sjölander, M. P. Tosi, and R. H. Land, Phys. Rev. B 1, 1044 (1970).
[8]P. Vashishta and K. S. Singwi, Phys. Rev. B 6, 875 (1972).
[9]F. Toigo and T. O. Woodruff, Phys. Rev. B 4, 371 (1971).
[10]C. M. Singal and T. P. Das, Phys. Rev. B 8, 3675 (1973).
[11]J. Čižek, J. Chem. Phys. 45, 4256 (1966).
[12]J. Čižek, Adv. Chem. Phys. 14, 35 (1969).
[13]J. Čižek and J. Paldus, Int. J. Quantum. Chem. 5, 359 (1971).
[14]J. Paldus, J. Čižek, and I. Shavitt, Phys. Rev. A 5, 50 (1972).
[15]F. Coester and H. Kümmel, Nucl. Phys. 17, 477 (1960).
[16]H. Kümmel, Nucl. Phys. A 176, 205 (1971).
[17]H. Kümmel and K. H. Lührmann, Nucl. Phys. A 191, 525 (1972).
[18]H. P. Kelly, Phys. Rev. 134, A1450 (1964); D. L. Freeman and M. Karplus, J. Chem. Phys. 64, 2641 (1976).
[19]H. J. Monkhorst, Phys. Rev. B 12, 792 (1975).
[20]C. M. Singal and T. P. Das, Phys. Rev. B 12, 795 (1975).
[21]N. H. March, W. H. Young, and S. Sampanthar, *The Many-Body Problem in Quantum Mechanics* (Cambridge University, Cambridge, 1967), Chap. 5.
[22]A. L. Fetter and J. D. Walecka, *Quantum Theory of Many-Particle Systems* (McGraw-Hill, New York, 1971), pp. 151–167.
[23]D. Shanks, J. Math. and Phys. 34, 1 (1955).
[24]L. Hedin, Phys. Rev. 139, A796 (1965).
[25]T. Zivkovic and H. Monkhorst (unpublished).